Analytical modelling of the ball pin and plastic socket contact in a ball joint

J C Watrin, H Makich, B Haddag, M Nouari, X Grandjean

Analytical modelling of the ball pin and plastic socket contact in a ball joint

J.C.Watrin[1, 2], H. Makich[1], B. Haddag[1], M. Nouari[1], X.Grandjean[2]

[1]LEMTA, CNRS-UMR 7563, Lorraine University, LARIOPAC : Laboratoire commun de recherche public-PME, LabCom – Vague 2 – 2013, GIP-InSIC, 27 rue d'Hellieule Saint-Dié-des-Vosges F-88100,France.

[2] Vosges Technologie, Innovation et industrie, VT2i, 77 rue de l'état Ramonchamp F-88160, France

Abstract

This paper presents an analytical approach to study the failure of suspension ball joints.This degradation occursat the plastic socket/ball pin interface and is considered as the result of the complex loading that undergoes the ball joint during its lifetime. The developed approach reproduces this loading by estimating both the contact pressure profileand the displacement field for the plastic socket elements.The contact pressure was identified for the studied ball joints after fitting with the numerical simulation results based on the real load cases and motion solicitations. The displacement field has been identified by parameterizing elements of the plastic socket at the contact interface according to the motion solicitations. Thereby, the plastic socket wear has been analyzed based on the modified Archard's law.A confrontation with experimental tests on an automotive ball joint was carried out. The analytical model predictedwell the localization of degradation zones on the plastic socket. It was highlighted in this study that the motion solicitations historyhas an effectonthe overall wear.

Keywords: Ball joint; Contact interface; Analytical modelling; Polymer; Wear

1. Introduction

Ball joints are mainly used in different guiding functions in the automotive hub carrier.For example, it is a part of the various components of the vehicle suspension system. This equipment must withstand complex loading on vehicle handling. Suspension ball joints (ball pin and spherical plastic socket) allow the articulation of the wheel around its vertical axis and manage the movement of the suspension system of the vehicle. They are considered as critical safety partsin the ground liaison. Theoperating conditions generate a cyclic loading causing a damage in the ball joints and hence a reduction of their lifetimes. Thus, different failure causes should be carefully analyzed in order to warrant that parts do not exhibit early deterioration.

Thereby, due to the contact confinement in the ball joint, some authors used the combination of finite element modelling with the modification of the ball socket surface, due to his interaction with the ball pin, to evaluate the wear in the running phase of the ball joint (e.g. Ejtehadi et al. [1]). A different resolution methodology has been used by Peyruseigt etal. [2] which developed an analytical method toevaluate the pressure profile inthe aeronautical ball joints resulting from themechanicalloading.Using analytical modelsas done by Ejtehadi et al. [1] can save more calculation time incomparison with finite element computations as conducted by Germaneau et al. [3]which moreover do not evaluate the wear in the ball joint.Indeed, both analytical and numerical modellingsdo not take into account the plurality of motions and load solicitations due to real road environment. Based onthe real measurementswithdrawn during the real driving conditions given by the company partner VT2i, it has been possible to predict the probability of failure in fatigue of a ball pin using FEA and analytical models(Kadhim et al. [4]).

In order to predict the wear evolution in a spherical ball joint, it is necessary to understand the tribological behavior of materials involved such as the POM/Carbon based steel. The identified phenomena that causes wear in POM/Carbon based steel is resulting from the abrasive and adhesive contacts. To predict the wear rate of POM/Carbon based steel, Wuet al. [5] have used the modified Archard's law.The time integration of this lawgives the wear accumulation (height) in the meshed contact zone. Using the same hypotheses, Pietrabessa et al. [6] and Maxian et al. [7] used the discretized Archard's law to predict wear in a hip prosthesis. In addition, Scholten et al. [8] and Ejtehadi [7-8] used a similar law in the automotive spherical ball joint.

Concerning the tribological behavior at the ball pin/plastic socket interface (usually carbon based steel/POM), an evaluation of the friction coefficient at different temperatures, sliding speed and shape geometry using different tribological tests has been performed by several authors, [9-12].Samyn et al. [9] analyzed the behavior of the 42CrMo4/POM couple using a cylinder plate tribometer test. In this study, the influence of sliding speed and load has been studied.by these authors. In addition,Benhabdallah et al. [11] compared different engineering plastics, derived from the Polyoxymethylene, and different coating surfacessliding against carbon based steel. The authors discussed the friction and wear evolution of the blended polyoxymethylene sliding against coated steel plates.

In the present study, the probability of the ball joint failure has been analyzed. An analytical model was developed to estimate the sliding distance and the pressure field on the ball socket using elasticbehavior of the material. Furthermore, several tribological tests have been performed to evaluate the friction coefficient and the wear rate under different loads and sliding speeds, representative of the global movement of the ball joint during its lifetime. The linear ball on plate reciprocating test has been preferred to the 'pin on disk'test. This is due to the alternative motion at the contact zone in the ball joint. Thus, the evaluation of the friction

coefficient has been done in the range of frequenciesand loads as in the real solicitation of the automotive ball joint. Coupling the wear rate, the pressure profileand the sliding distance field of the socket, the wear resulting from the mechanical solicitation has been estimated. Finally, several real tests have been carried out on the ball joint to compare the experimental and predicted wear fields.

2. The proposed analytical model

2.1. Ball joint System

Suspension ball joints systemsallow the articulation of the wheel around its vertical axis and manage the movement of the vehicle suspension. This induces cyclic loading on the ball joint components during his lifetime. It will receive alternative or constant solicitation, and at the same time will rotate around the ball joint axis. The suspension ball joint failure, resulting from the load and motion solicitation, is located at the spherical contact interfacebetween the ball pin and the ball socket (see Figure 1a). The ball pin is made of a carbon based steel sphere which can be linked to another part of the suspension system and receive torque and load solicitations from the road. The second component is the polymer based ball socket. This component is directly inserted to the housing,in clear grey in Figure 1,which is also made ofcarbon based steel. The studied area is the interface between the ball pin and the ball socket.

The proposedanalytical model is based on the discretization of the ball joint contact interface and the evaluation of the sliding distance, contact pressure and wear during simultaneous loading and motion.The aim of the modelling is to estimate the geometry modification of the ball joint contact interface resulting from the cyclic loading.

During the ball joint lifetime, load and motion solicitations are depending on the road type (country road, highway etc.). To predict and evaluate the wear resulting from each road

configuration, it is necessaryto consider the impact of the road on the global movement of the ball joint. Load and motion solicitations are defined as input sequences of the analytical model. Each sequence represents a road configuration which influences the following parameters: the load case$\boldsymbol{F_{axial}}$,tilting$\boldsymbol{\varphi_i}$and rotation $\boldsymbol{\theta_i}$ limit angles, tilting $\boldsymbol{f_t}$and rotation $\boldsymbol{f_r}$ frequencies, and the number of cycles of each road configuration $\boldsymbol{n}$. A sequence is defined according to these parameters,as follow:

$$S_p = \{F_{axialp}, \varphi_{ip}, f_{tp}, \theta_{ip}, f_{rp}, n_p\} \quad (1)$$

One cycle is defined as theglobal movement of tilting and rotation which is duplicated $\boldsymbol{n}$ times and that is the characteristic of the ball joint behavior in a typical road configuration. Each test modelling is defined with a certain number of sequences$\bar{\bar{S}} = \{S_1, S_2, \dots, S_{p-1}, S_p\}$ which contains $\boldsymbol{n_p}$ cycles. In the following, the model is explained considering one sequence $\boldsymbol{Si}$ with a constant applied load$\boldsymbol{F_{axial}}$.

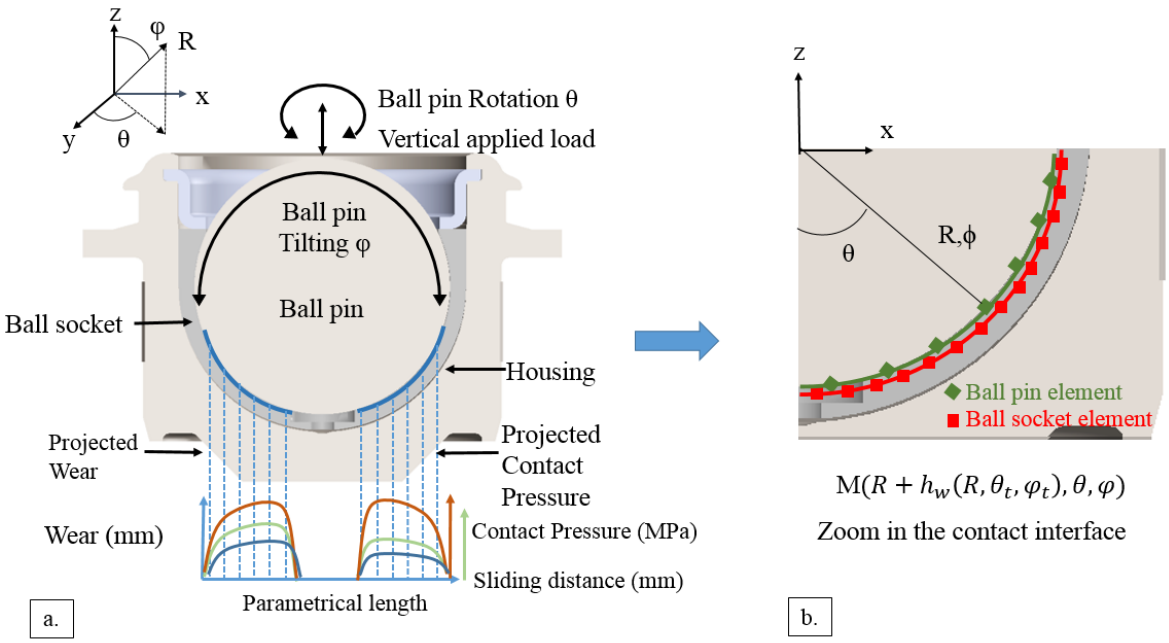

Figure 1.A schematic view of the ball joint. (a)- Ball joint load and motion solicitations.(b)- Elements of the ball joint and zoom in the contact interface.

All calculations have been carried out on the global projected ball socketsurface (see Figure 1a). The ball socket has been meshed with 3600 elements and the ball pin with 1680 elements (Figure 1b). Each element is defined in the ball socket coordinate system as follow: $(R + h_w(R, \theta_t, \varphi_t), \theta, \varphi)$, which $h_w(R, \theta_t, \varphi_t)$ is the wear depth resulting from abrasion at time t, θ is the first angle coordinate of the sphere,φ the second angle coordinate on the sphere, and R is the ball pin radius. The wear evaluation, pressure and sliding distance have been carried out at each cycle.To evaluate the wear resulting from the pressure profile and the global movement of the sphere, it is needed to evaluate first the sliding distance field on the ball socket.

2.2. Wear evaluationatthe ball pin / plastic socket interface

The ball joint failure is the consequence of the interface degradation between the ball socket (POM) and the ball pin (Steel). This wear is induced by two mechanisms, the abrasion of the ball socket surface withthe ball pin and plastic deformation due to the axial load. Only abrasion wear contribution was considered in this study. The abrasion effect resulting from the material couple can be modelled using the Archard law. The latter is widely used to predict the wear behavior of loaded surfaces. Ejtehadi etal.[1] have been used this modeling to predict the abrasive contribution tothe contact interface modification with the POM/Carbone based-steel couple. The Archardformulation is presented as follow:

$$V = kF_n s \tag{2}$$

which $\boldsymbol{V}$ is the worn volume in mm^3, $\boldsymbol{F_n}$ the normal applied load in N and $\boldsymbol{s}$ the sliding distance in mm, and $\boldsymbol{k}$ the wear coefficient in mm^2N^{-1}.

To implement this equation in the proposedmodel, it is necessary to discretize this equation. Thus,themodified Archardlaw is often used by several authors, [5-7] for the evaluation of the wear depthgiven by the following equation:

$$h_w(R,\theta_t,\varphi_t) = kL(R,\theta_t,\varphi_t)p(R,\theta_t,\varphi_t) \quad (3)$$

where $\boldsymbol{h_w}(R,\theta_t,\varphi_t)$,in mm, is the evolution of radial dimension of the ball socket surface during one cycle, $\boldsymbol{k}$ in mm^2N^{-1} is the wear coefficient resulting from experimental tests, $\boldsymbol{L}(R,\theta_t,\varphi_t)$, in mm, is the sliding distance of the ball socket point during the cycle, and$\boldsymbol{p}(R,\theta_t,\varphi_t)$, in MPa,is the normal pressure applied on the ball socket element.

2.3. Sliding distance evaluation for the ball socket elements

The modifiedArchard lawis used in the analyticalmodel to predict the new ball socket geometry resulting from the load and motion solicitations. First of all, it is necessary to evaluate the global sliding distance field and then the pressure profileinthe contact interface resulting from the ball pin load and motion solicitations. To evaluate the sliding distance field of each sequence, it is important to understand the global ball pin motion in the ball socket coordinate system. Pietrabessa etal. [5] modeled the global movement of a hip prosthesis in the spherical coordinate system. All model calculationshave to be doneinthe projected contact interface so it is necessary to adapt the movement from 3D to 2D and discretize the movementin time. Defining a time incrementtbetween $t_i$andt_f, which are respectively the beginning time and final time of one cycle, it is possible to evaluate the global ball pin motion in the spherical coordinate system of the ball socket.The projected arc $l(M_tM_{t+1})$of a point M in the ball pin and his projected trajectory between $t_i$and $t_{i+1}$is given by the following equation:

$$\mathrm{l(M_tM_{t+1})} = \begin{Bmatrix} \theta_{t+1} = \mathrm{R}\left(\delta_{jt}(t)\theta_t - \theta_i\right)f_r\delta_{kt}(t)t \\ \varphi_{t+1} = \mathrm{R}\left(\delta_{jr}(t)\varphi_t - \varphi_i\right)f_r\delta_{kr}(t)t \end{Bmatrix} \quad (4)$$

which $\delta_{ji}(t)$ and $\delta_{ki}(t)$ are parametric functions synchronizing the ball pin movement of rotation and tilting,simultaneously.

Let's simplify the global movement of the ball pin. If the ball pin does not rotate and tilt simply between two positions $-\varphi_i$ et φ_i at the frequency f_t, the global movement of the ball pin is described by this equation:

$$\mathrm{l}(\mathrm{M_t M_{t+1}}) = \begin{Bmatrix} \theta_t = 0 \\ \varphi_t = \mathrm{R}(\varphi_t - \varphi_{t+1})\mathrm{f_r} t \end{Bmatrix} \quad (5)$$

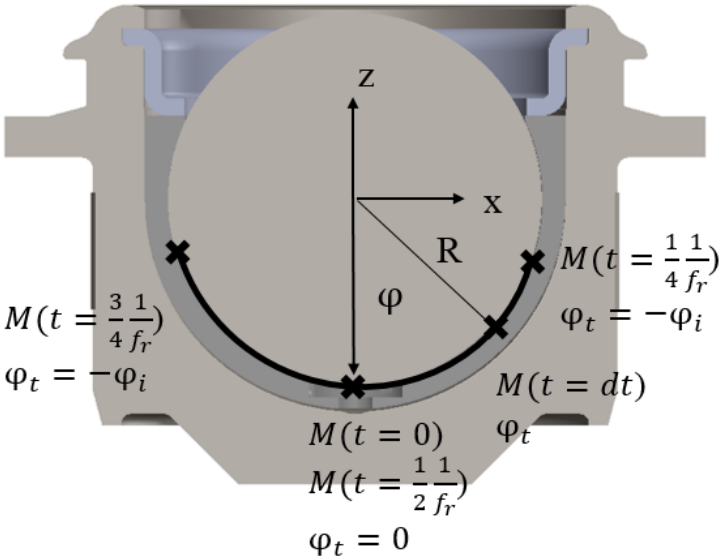

Figure 2.Motion representation at the interface ball pin / ball socket:One cycle with tilting $\pm\varphi_i$at the frequency $f_t$without rotation:$\theta_t = 0$

Using the ball pin motion modelling, the global trajectory of each point of the ball pin can be assessed on the ball socket contact surface. Then, the number of times, when each ball pin element is detected by the ball socket element, is evaluable. So, integrating on each element of the ball socket between $\mathrm{t_i}$ and $\mathrm{t_f}$the number of ball pin elements detected during this time period, the eulerian field of passage $D(R, \theta_t, \varphi_t)$on the ball socket surface can be estimated by the following equation:

$$D(R, \theta_t, \varphi_t) = \int_t \iint_{M \epsilon S} \varepsilon_i(l(MM_u), R, \theta_u, \varphi_u) dS dt \quad (6)$$

Thus, using this equation and themaximum sliding distance$L_{max} = l\left(MM_{t_f}\right)$ of each point of the ball pin on the ball socket, the Eulerian sliding distance field on the contact area can be evaluated by the following expression:

$$L(R,\theta_t,\varphi_t) = \frac{D(R,\theta_t,\varphi_t)}{\max_{M\in S} L(M)} L_{max} \quad (7)$$

2.4. Evaluation of the pressure profile

During the process, the ball joint mainly undergoes an axial loading. To predict the failure of this component, it is necessary to determine the pressure distribution induced in the contact interface between the ball pin and the ball socket.The pressure evaluation has been previously predicted by Germaneau et al[3] in the case of aeronautical ball with the following equation:

$$P(\theta,\varphi,R,F_{axial}) = P_{max}(R,F_{axial})\cos\left(\frac{\theta}{\theta_i}\frac{\pi}{2}\right)\cos(\varphi) \quad (8)$$

which $\boldsymbol{P}$ is the normal pressure in MPa,$\boldsymbol{P_{max}}$ is the maximal pressure in the contact interface, $\boldsymbol{F_{axial}}$ is the normal axial load, $\boldsymbol{\theta_i}$and$\boldsymbol{\varphi_i}$are the rotation and tilting limit angles,respectively.However, Germeneau used this type of equation considering metal-on-metal contact (steel/steel contact), contrary to suspension ball joint with a POM/Carbon based steel contact. Moreover, the contact angle is limited in two directions in the suspension ball joint which is not the case ofaeronautical ball joints. Due to the design and material difference between the aeronautical ball joints and the suspension ball joints,Equation7 has be adapted.Inthis work, thefollowing equation 8 which corresponds to the case of our studywas identified.Eq.8wasused to evaluate the pressure profile and fitted with numerical simulations:

$$P(\theta,\alpha,R,F_{axial}) = P_{max}(R,F_{axial})\left(\frac{\sin\left(a\frac{\theta}{\theta_{lim}}\right)\sin\left(a\frac{\alpha}{\alpha_{lim}}\right)}{b\frac{\theta}{\theta_{lim}}b\frac{\alpha}{\alpha_{lim}}} + c\right) \quad (9)$$

The numerical pressure estimationwas carried out using finite element analysis. Two components (ball pin and ball socket) are considered in the numerical simulations and“surface to surface”contact was used. Tetragonal elements are used in both elements. Material linear behavior was used for the carbon based steel and for the POM (ball socket). Three numerical simulations wereperformed with different applied loads and different ball pin diameters to fit numerical simulations and analytical results. The test configurations were taken from real suspension ball joint load solicitations in the automotive industry given by our partner VT2i and are presented in Table 1.

Table 1. Test hypothesis for numerical simulation

Test configuration	Ball pin diameter (mm)	Normal Load applied (N)
Test 1	25	5840
Test 2	16	1500
Test 3	19	5000

The results of numerical simulations and the fitted numerical analysis (equation 8) are plotted in Figure 3with parameter a=5, b=6, and c=0.5. The parametrical length is a θ constant meridian of the ball socket contact interface. The fitting has been performed using the mean squared error reductiontechnique.

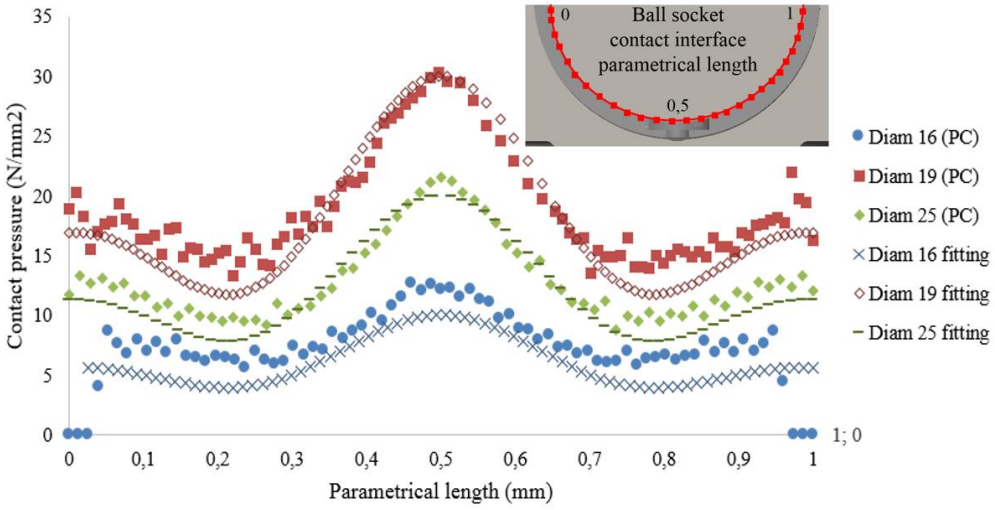

Figure 3.Analytical model and numerical simulation fitting using a linear behavior of the ball socket.

Figure 3 shows the evolution of the pressure profile on a 180° arc of the ball socket for three different geometries. The static applied load direction in the finite element model follows the Z axis. It can be observed a pressure pic in the center of the ball socket (parametrical length = 0.5).

In theseload cases, the force wasapplied in the direction of the ball pin symmetry axis at zero position ($\theta = 0, \varphi = 0$). In addition, considering the ball pin global motion (tilting and rotation motion), the axis of the ball pin will not coincide with the ball socket symmetry axis at any time.Thus, during one cycle of movement, the ball socket pressure will change. Assuming in the modethat during one cycle l, the pressure is time constant, it is necessary to mean the pressure evolution resulting from the ball pin motion and to use a new analytical model(Figure4).In addition, considering that in each cycle and in each element, the pressure will be update, Eq 8 need more than 10 calculations per element to evaluate the final pressure. To limite the CPU time with a large number of cycles,a constant based pressure profile has to be used in the model given by the following equation:

$$P(\theta, \alpha, R, F_{axial}) = \frac{\gamma F_{axial}}{S(t)} \tag{10}$$

where $\boldsymbol{F_{axial}}$ is the applied load around the ball stud axis, $\boldsymbol{\gamma}$ is the fitting coefficient, and $\boldsymbol{S}$ is the contact interface surface.

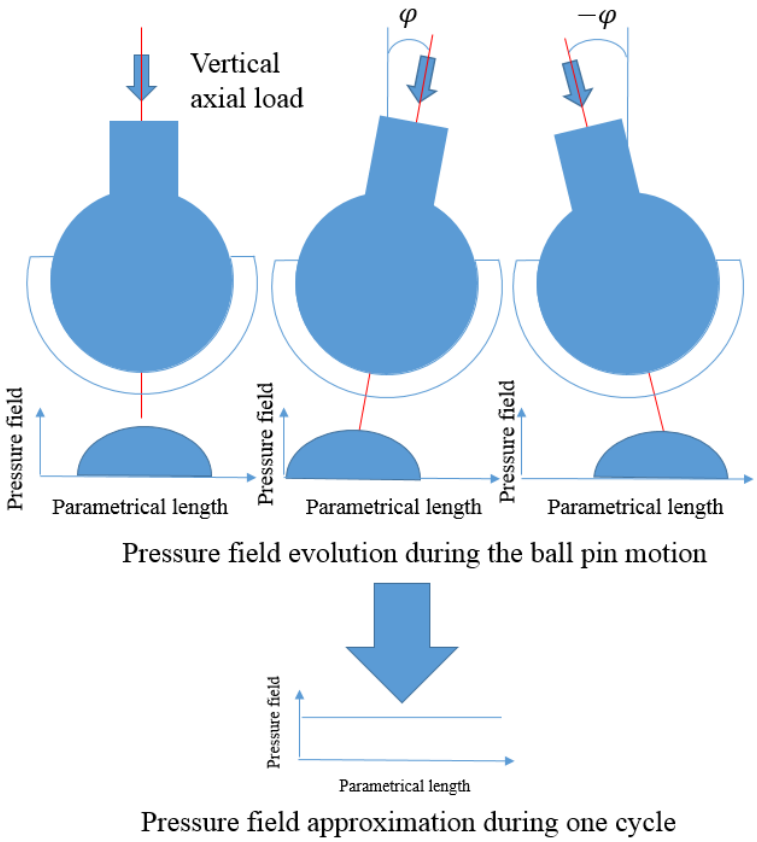

Figure 4. Pressure approximationpercycle.

Comparing the results of pressure used in the numerical simulation with the pressure fieldusing the two differentanalytical equations (Eq.9 and Eq.10), the mean pressure can be compared and given Table 2. From this table, the parameter $\boldsymbol{\gamma}$ is identified with the value 2,08.

Table 2. Mean pressure of analytical modelling and numerical simulation comparison.

Configuration	Ø16mm / 1500 N	Ø19mm / 5000 N	Ø25mm / 5840 N
Mean pressure (Numerical simulationin MPa)	7.4	18.5	12.9
Mean pressure Eq. 8 model (MPa)	6	17.3	12
Mean pressure Eq. 9 model (MPa)	7.8	18.3	12.4

In the following the pressure profile used in the analytical modelling is estimated byEquation 10. The result of this approximation is to misevaluate the resulted wear on the ball socket borders. Indeed, the pressure field increases at the borders of the contact interface and close to

the grooved surface. This evolution was not taken into account in this model. In addition, at the center of ball socket (φ=0), the estimated pressure is smaller than the more representative pressure profile (Eq.9), so the estimated wear can be underestimated in the concerned zone.

3. Experiments and details

Several tribological tests were carried out on the POM/Carbon based steel contact to evaluate the wear coefficient involved in Archard wear law. Thesetests were performed at different loads and different sliding speeds. Considering the ball pin motion in the ball socket at a small scale (see Figure 5c), the reciprocating test seems to be a better solution than other closed tribometer test such as 'Pin-on-disc' test. Indeed, to have representative results, ithas been considered a closed test instead of an open one.The POM/Carbon based steel reciprocating test has been performed by several authors,[9-12],but not in the range of our frequenciesand loads. In addition, the effect of the wear coefficient evolution has not been evaluated before for this range of loads and sliding speeds. The test was carried out with the tribolab apparatusmanufactured by Brücker. The pin-on-plate test configuration is synthetized in Table 3.The stroke of the reciprocating test is about 18mm.

Table 3. Pin and plate materials and dimensions description.

	Pin	Plate
Material	POM	Carbon based steel
Diameter/dimension	Ø6.35mm	43.18mmx30.48mmx5.08mm
Roughness	Ra : 0.1	Ra : 0.1

To evaluate the effect of the sliding distance, sliding speed, and load on the wear coefficient, 2 loads (10N and 20N), and 3 sliding speeds (10mm.s^{-1}, 20mm.s^{-1}, 30mm.s^{-1}) have been used. These values were chosen after comparing different real load cases and motion solicitationstaken from the automotive industry (VT2i Company).

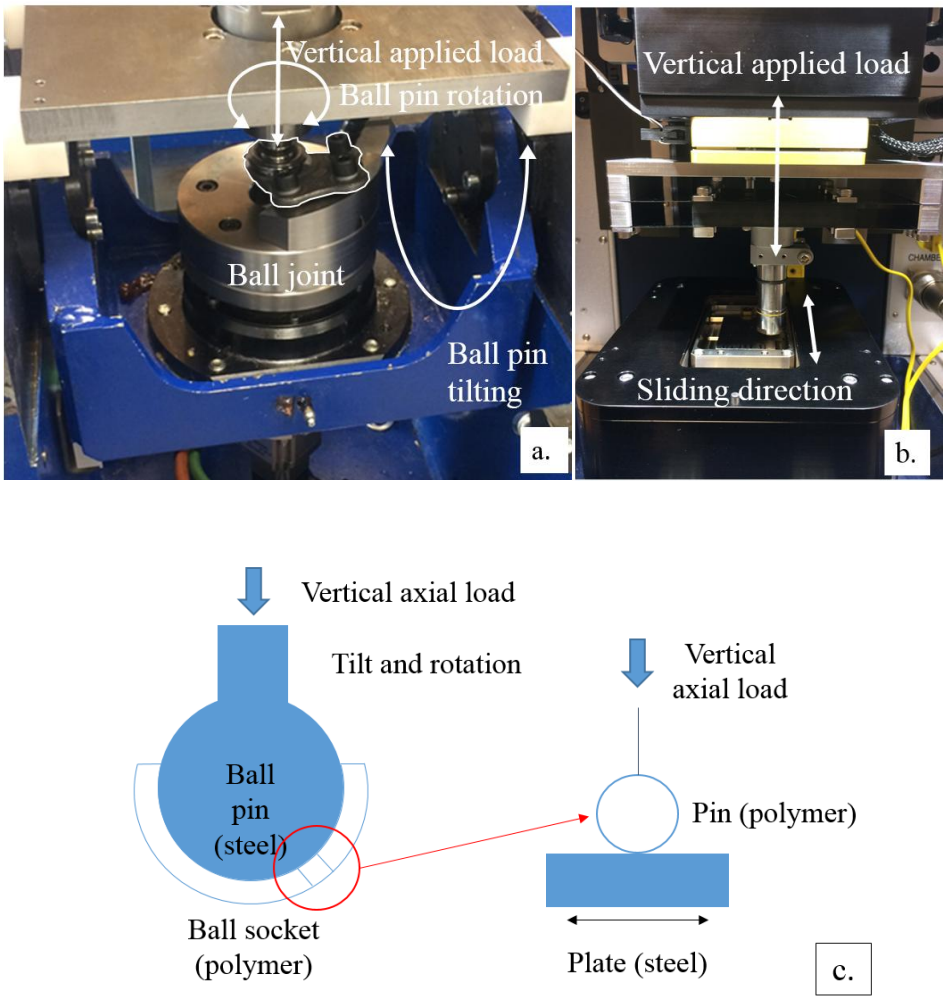

Figure 5.a. Large-scale ball joint wear test, industrial test. b. Small-scale test done in the laboratory (Reciprocating tribometer) c. Large-scale to small-scale test transition.

Further investigations were performed on large-scale test called wear test using the industrial platform of our partner VT2i. A 900daN axial forceand rotation (±15° at 1Hz)) and tilting (±10° at 0.5Hz) movement is applied to the ball pin around the Zero position during 113 hours (Figure 5a). After the test, the ball socket wear was measured by a laser line sensor and the final shape of the ball socket was compared with the analytical final shape (calculated by the model).

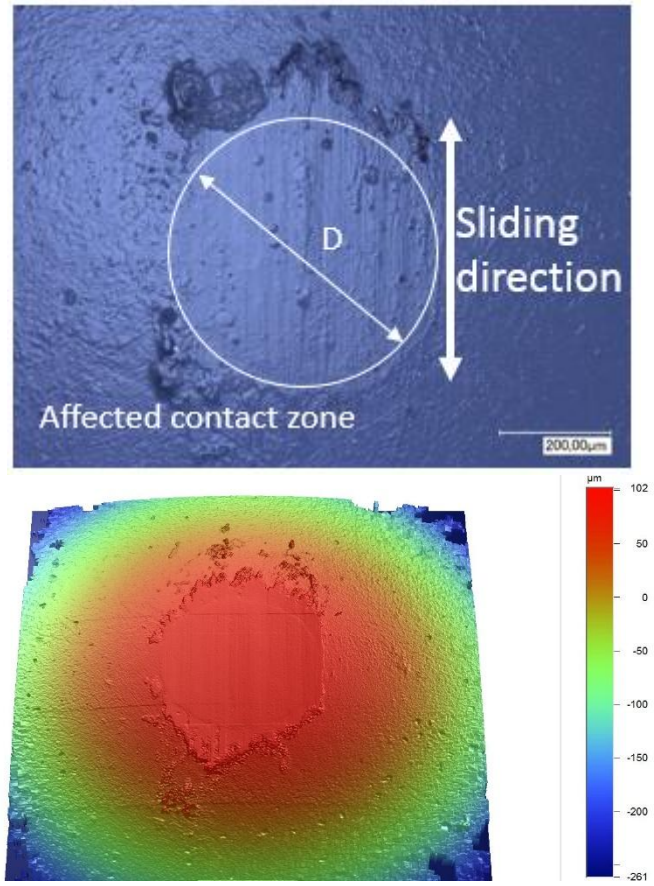

Figure 6 : Wear characterization during tribological tests. Test conditions: 10N-20mm/s-2100 cycles. ()

Normal and tangential loadshavebeen recorded during the test and the wear volume was measured after the test with an optical microscope.The affected contact zone, resulting from the alternative test on the pin, reproduces the local contact shape of the ball pin/ball socket contact. Two different phenomena can be highlighted, striations and flanges. Striations are due to the abrasive behavior of the material couple as seen in Figure 7. On the other hands, flanges indicate that plastic deformation can occur during the alternative tests. The mass transfer phenomena have been highlighted in the literature in a certain range of sliding speeds and load cases, [9-12].The evaluation of adhesive contact in the POM/steel contact is to be related with a high increase of the friction coefficient. No shape change was noticed(see Figure 8), so the adhesive effect does notappear in this range of sliding speeds and loads, only abrasive and plastic deformation appear.Based on the Archard law, it is possible to characterize the wear behavior of the POM/Steel couple. The wear volume was evaluated

based on the diameter measurement of the truncal sphere removed during the test. All diameters were measured and the influence ofthe sliding distance on the wear coefficient is plotted in Figure 7.

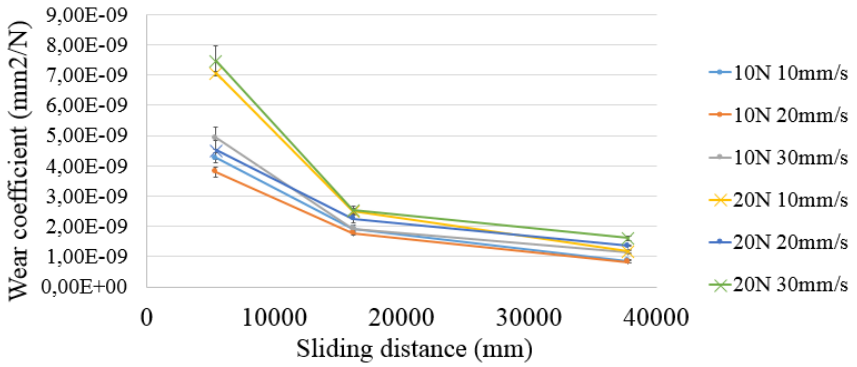

Figure 7. Evolution of the wear coefficient with the applied force, sliding distance and sliding speed.

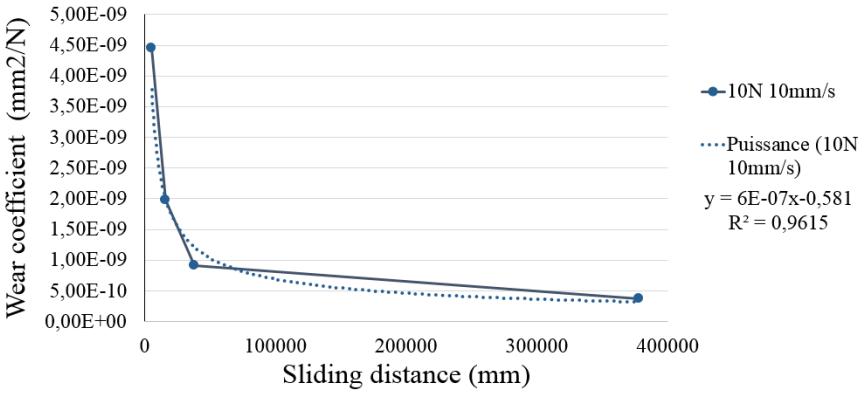

Figure 8. Evolutionof the wear coefficient with the sliding distance at 10N and 10mm/s.

The sliding distance performed during the small scale tests is different compared to the number of cycles used in our model (40minstead of 4km). It wasfound in the literature that the wear coefficient during the long life test is assumed to be constant. But before the steady-state phase, a transient phase has to be considered. When the number of cycle is above 50m, the wear rate is high, decreases and don’t stabilize, which is representative of thetransient phase. The force and sliding speed influence on the wear coefficient is noticeable above 20m. But after 20m, the force effect on the wear coefficient decreases. By fitting the curve, it is possible to evaluate a relationship between the wear coefficient and sliding distance.

Compared with our large scale test, the most representative small scale test is 10N-10mm.s^{-1}. In order to better evaluate the variation of the wear coefficient during a longer sliding distance, it has been decided to evaluate the wear coefficient at 400m (8 hours test). The results are plotted in Figure 8. After 50m, the wear rate decreases and appears to be constant, which characterizes the steady state stage of the curve.Using this curve, it is possible to determine a relation between the wear volume and the sliding distance by using the mean squared reduction methodology:

$$k = 6.10^{-7} l^{-0.580} \tag{11}$$

This equation assumes that at an infinite cycle, no wear effect will happen, but considering a large scale test and applying 4km as l, k reaches 10^{-11}mm^2.N^{-1} which explains the stabilization phase. At first approximation, we assume that the wear coefficient is constant in our model and equal to 3.10^{-10}mm^2.N^{-1}.

4. Results and discussions

4.1. Application of the model

The inputs of the model are (i)- the number of sequences and (ii)- the ball joint geometry (ball pin radius, and ball socket grooved geometry). Taking into account the number of sequences, the algorithm computes, cycle per cycle, the wear ball socket deformation, and updates the ball socket geometryEquation 3and the pressure profile(Equation 10) resulting from thenew contact interface shape and load solicitations. After finishing a sequence, a new sequence defined as a new load and motion solicitations will be computed and all the contributions of these solicitations will be summed.The global algorithm is detailed in Figure 9.

Using this algorithm, the contribution of all road types can be taken into account considering different sequences as input and the model can simulate a large-scale test on ball joints and

predict the effect of wear on the ball socket geometry during his lifetime using correct tribological input.

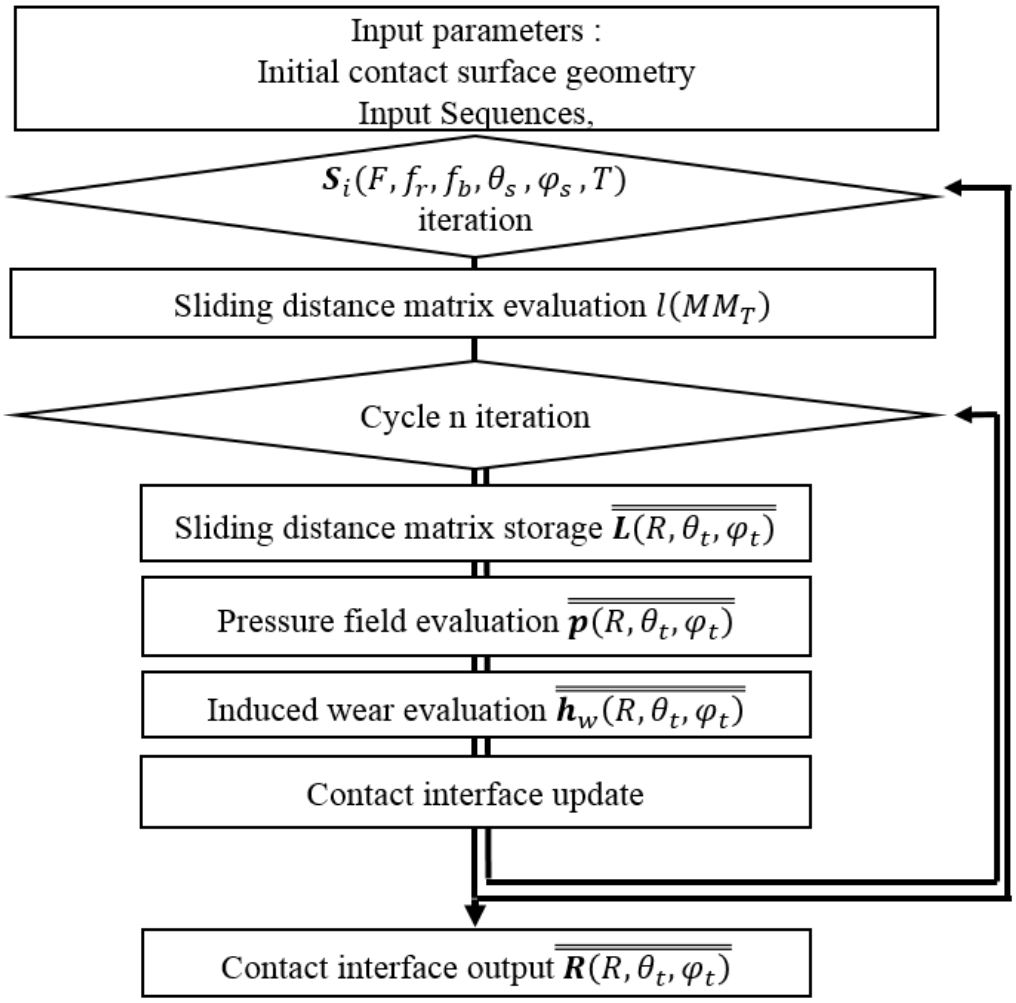

Figure 9. Analytical model algorithm

4.2. Analysis of the local parameters

The model has been performed based on the same parametersof the ball joint large–scale test (wear test): The applied load is about 900daN. The applied motion was ±10°tilting angle at 0.5Hz and ±15° rotation angle at1Hz.

The sliding distance is evaluated at each sequence. In this test, only one sequence (One type of motion) is used and the sliding distance field is plotted in the following Figure 10. A

θ constant element line has been drawn and the sliding distance field is plotted in only ¼ of the ball socket diameter.

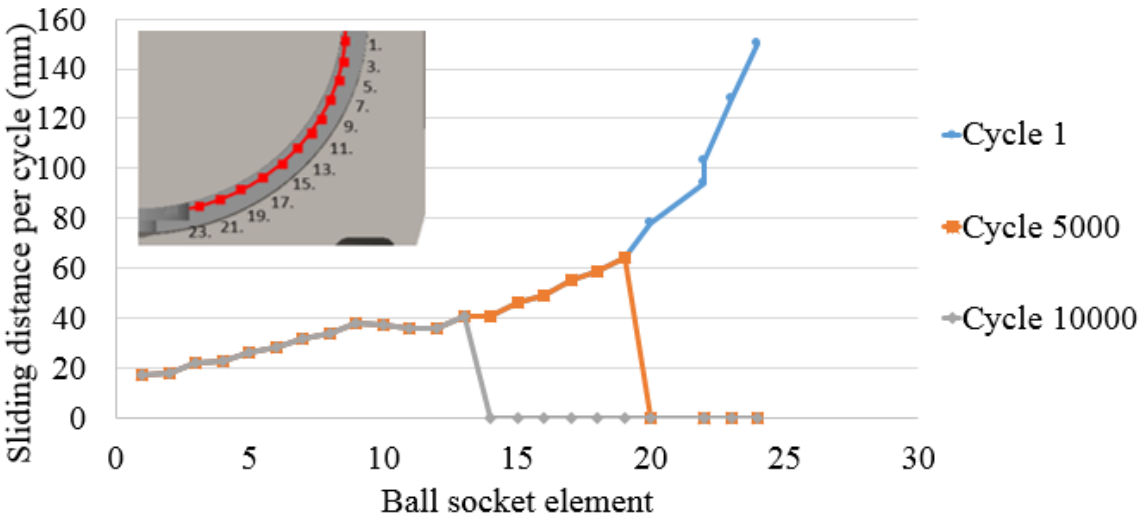

Figure 10. Sliding distance in different elements.

The large sliding distance value islocalized close to the point of the applied load. It is due to the fact that the initial position of the ball pin is θ=0 and φ=0 and that the motion solicitation is an alternative motion centered on the initial position. As a result, the sliding distance of points located on the center of the ball socket is higher and will decrease to zero in the direction of the ball socket boundaries. Moreover, the sliding distance field remains the same as the initial one. When the number of cycle increases, the elements number 19-25 reaches the contact limit and no more pressure will be applied to these points. As a consequence, the sliding distance during the 5000^{th} motion will fall to zero on these elements and remains the same as cycle 1 for the other one. When the number of cycle increases, more and more points will be deactivated and the sliding distance field for the cycle n will decrease.

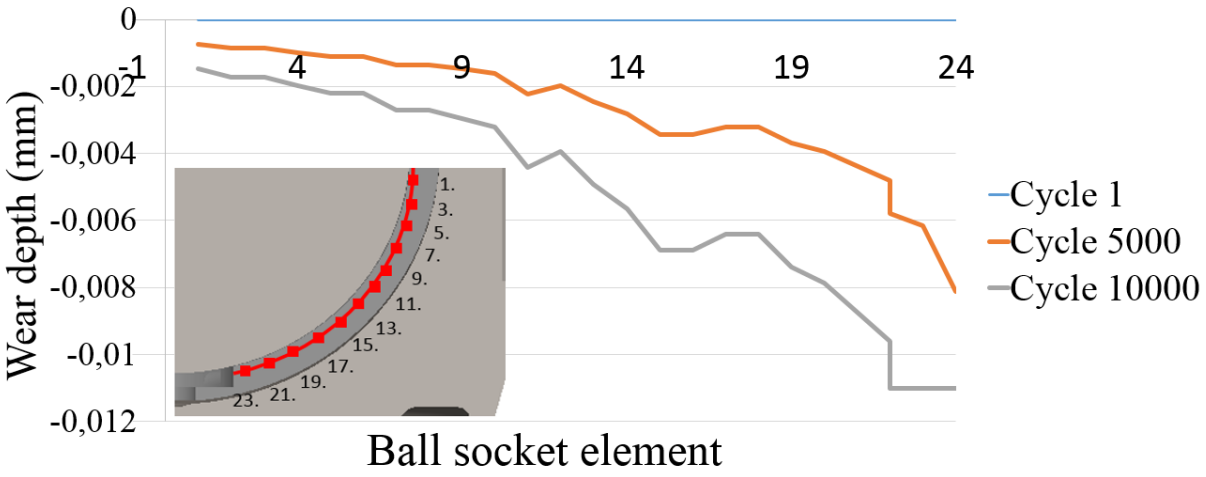

Figure 11. Geometry evolution of the ball socket at last cycle.

The large sliding distance value islocatedclose to the point of the applied load. Concerning the pressure field which is assumed constant as at the beginning for the first cycle, the wear resulting for the first cycle (Figure 11) will be higher in the center of the ball socket and will decrease until the frontier of the ball joint is reached. The wear repartition until the contact saturation limit is reached and dictated by the sliding distance field. If the pressure profile shape changes, it will affect the wear depth field behavior. The wear depth of the complete contact interface line at θ=0 constant and his evolution during the number of cycles have been plotted in Figure12.

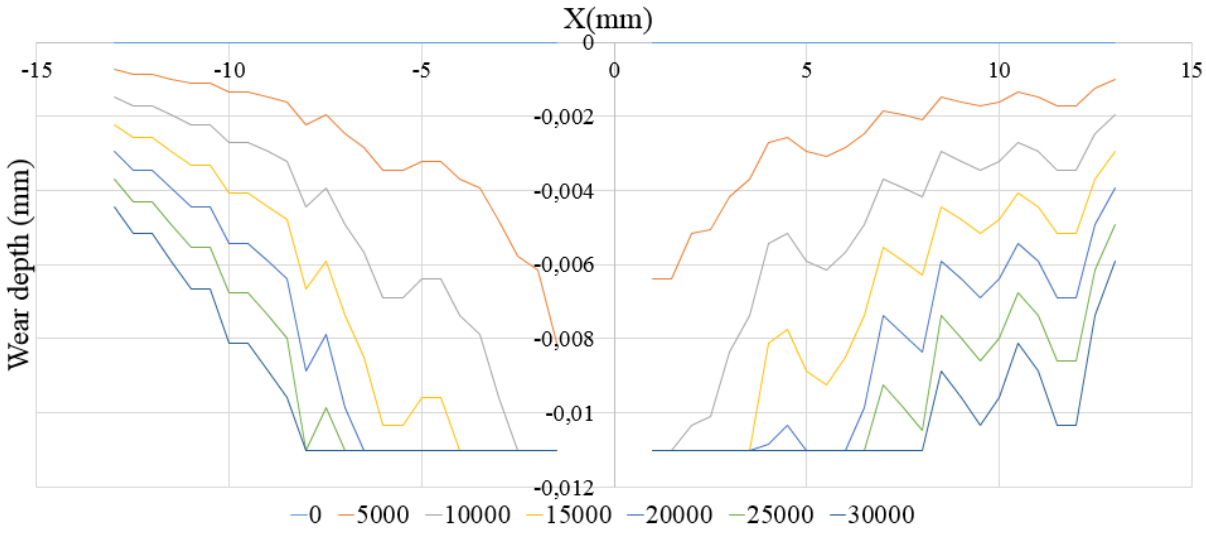

Figure 12Geometry evolution during different cycles.

The graph seems to be symmetrical. This is due to the fact that the motion solicitation is centered on θ=0 and φ=0 and that the motion solicitation is alternative.

Following the number of cycles, when the wear induced in the ball socket geometry exceeds the elastic deformation criteria, there is no more contact between the ball socket and the ball pin, and the pressure at these elements is equal to zero. For example, at 10000 cycles, the saturation begins at X =-2mm. At 15000 cycles, the saturations range increases and reaches -4mm. Step by step, the wear depth is getting more and more uniform in all the surface of the ball joint due to the contact test saturation criteria. Indeed,the wear depth achieves 0.012mm which the limit displacement value is resulting from the input applied pressure using a linear elastic behavior. After this value, there is no more contact on this area. Then when all the pressure will be equal to zero, a new contact surface will be created and wear will be reinitiate at the center of the ball socket.

4.3. Analysis of the ball socket wear

The tested ball socket geometry (Figure 13a) after wear test has been measured (using a laser acquisition) to evaluate the modification of the contact interface and has been measured using a profilometer to detect the wear phenomena. Figure13 shows striations, which are not located in the same direction. Abrasive curves can be detected. Compared with Figure 6 used in the case of small scale tests, a global trajectory motion is not detectable. Indeed, the large scale test has been performed using simultaneous rotation and tilting angle, so the global trajectories of ball pin points are not parallel and must be curves.

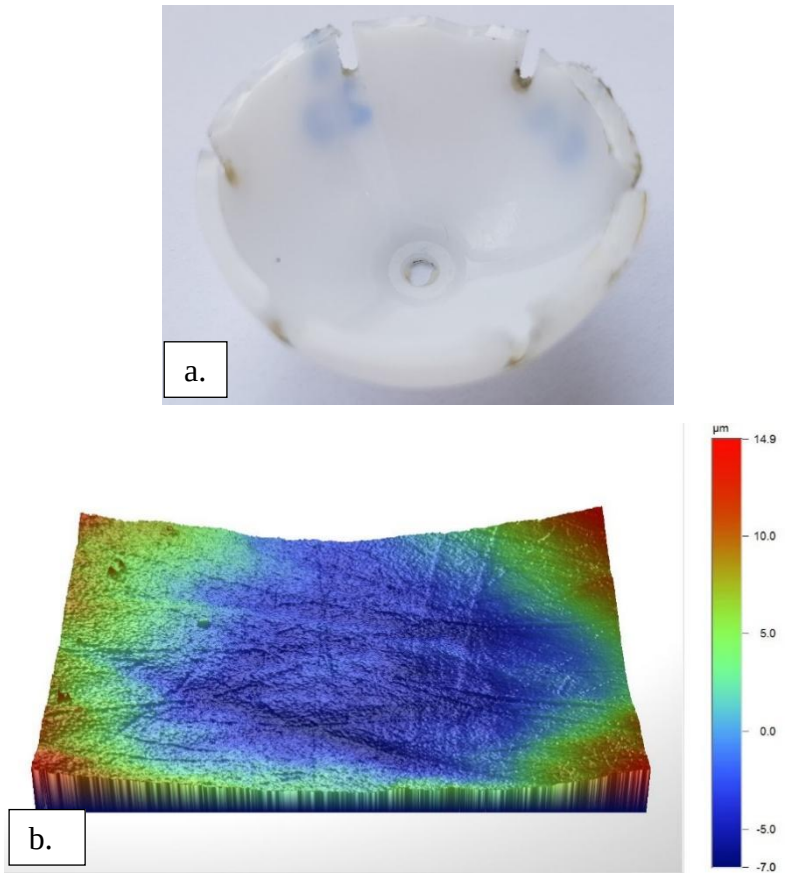

Figure 13a. Ball socket design after wear test. b. Analysis of the ball socket contact interface using a Brüker tribometer.

The modification of the ball socket geometry is plotted in Figure 13 with the analysis of the geometry evolution results. Three different curves are plotted: The first one is the ball socket that has not performed the large-scale test. The second one is the ball socket that has performed the wear test. The third curve is the analytical results. They have been placed considering that at the upper borders of the ball socket, the wear depth can be assumed to zero and the three points of the three curves can be confounded.

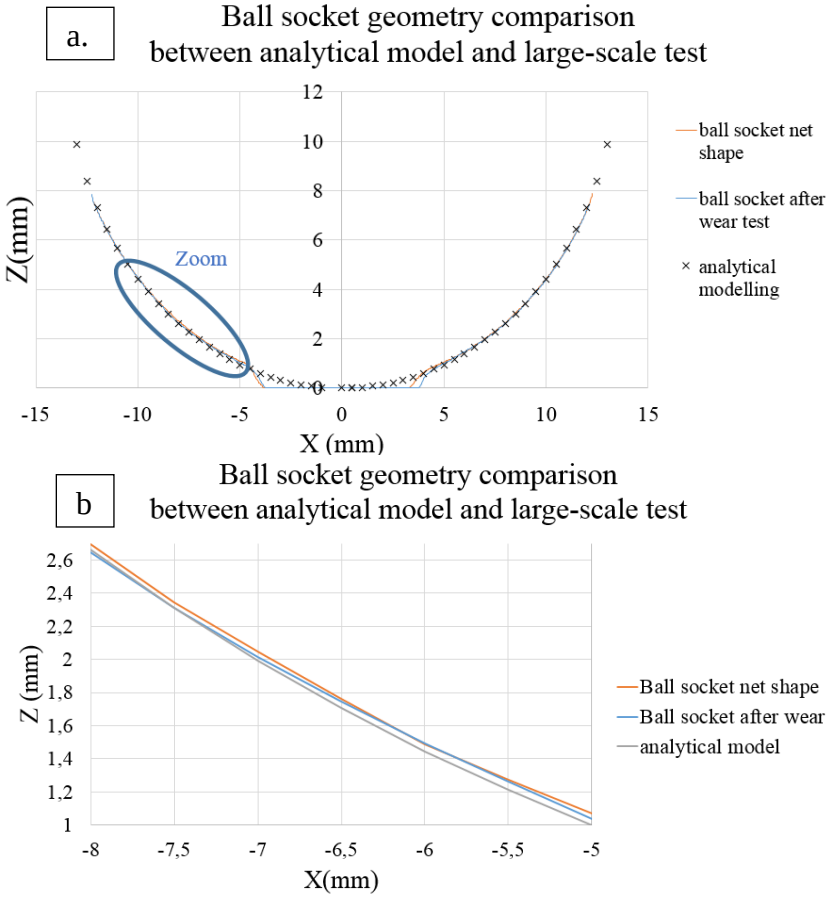

Figure 14a. Analytical model and large scale test on the global contact interface b. Zoom between 5 and 8 mm.

In the range from -5 to 5 mm, the ball socket has a grooved surface and no contact is created between the ball pin and the ball socket. The analytical model has the same shape as the ball socket after wear test. From –10mm to -7mm, the shape has to be close to the ball socket after wear test. From -7mm to -5mm, the analytical model wear increases and is higher than the ball socket after wear. The analytical model overestimates the wear in the global contact interface. This is due to the fact that the coefficient of friction has been considered as a dry contact. Indeed, due to the grooved ball socket geometry, the grease repartition in the ball socket is not uniform and will change throughout his lifetime. One solution can be considered to perform new tribological tests using lubrication and to create a contact surface based linear equation between lubricated and dry contacts.

In addition, the wear coefficient has been established based on the pin on plate test. During the cycle, the global pressure in the pin contact interface decreases and affects the wear coefficient. Some tribological tests have to be carried out to validate the wear coefficient using a different geometry.

The large scale analysis has been performed on real ball joint and very low wear depth was measured (about 0.01mm maximum). Some analysis have to be performed with higher number of cycles to confirm the coherence of analytical and large-scale geometry modification.

5. Conclusion

In this paper, an analytical modelling of the ball pin and plastic socket contact in a ball joint has been developed to estimate the wear of plastic socket, which is the component of the ball joint that fails first. The following conclusions can be drawn:

(1) From tribological tests performed on the POM/carbon based steel,the wear coefficient law was identifiedin dry contactat different sliding speedsand loads. This law covers the beginning and the steady state periods.For the steady state period, the wear coefficient is about 3.10^{-10} mm^2N^{-1}.

(2) An adaptive contact pressure profilemodelling from aeronautical ball joint was found for the automotive ball joints after fitting with FE simulations based on real load cases.

(3) The analytical modelling, including the wear coefficient as input in the modified Archard law, enables to evaluate the ball socket contact interface geometry modification resulting from a constant applied load at the beginning of the large-scale wear test.

(4) The model overestimates the geometry modification, due to wear, and some correctionsare required. Thismainlyconcernsthe identification of the correct wear coefficient and the real pressure distribution.

(5) So, to improve the analytical model, further tribometer tests should be performed with a higher sliding distance and with another pin design. Also, further large scale tests should be performed at higher number of cycles and higher load to validate the analytical model.

(6) It should be noted the powerful of such analytical approach, which is able to provide in reasonable CPU time the wear distribution in the ball joint for quasi-real loading cases. Such tool can be used to dimension critical contact components of ball joints.

6. Acknowledgements

The authors wish to thanks the industrial partners VT2i, and the financial partners RÉGION GRAND-EST(France) and FEDER (Fonds Européen de Développement Régional) which have made this research possible.

References

[1] M.H.Ejtehadi,H. Klaus, S.Sommer, H.Haensel, J.Scholten, Running-in phase of spherical chassis joints—identification of the main influence parameter and implementation in a wear simulation tool,*Int J Adv Manuf Technol* (2011) 55-983

[2] F. Peyruseigt, S. Mistou, O. Dalverny, M. Canadas, B. Jullière, M. Karama, Détermination et optimisation des pressions de contact dans les rotules par la méthode de flexibilité,*8ème colloque national en calcul des structures*. Giens. (2011)

[3] A. Germaneau, F. Peyruseigt, S. Mistou, P. Doumalin, J.-C.Dupré,3D mechanical analysis of aeronautical plain bearings: Validation of a finite element model from measurement of displacement fields by digital volume correlation and optical scanning tomography, *Optics and Laser in Engineering*, 40 (2010) 676-683

[4] N.A. Kadhim, S. Abdullah, A. Ariffin *Effective strain damage model associated with finite element modelling and experimental validation*International Journal of Fatigue 36 (2012) 194-205

[5] S. Wu, J. Hung, C. Shu, the computer simulation of wear behavior appearing in total hip prosthesis, *Computer Methods and Programs in Biomedicine* 70 (2003) 81-91

[6] R. Pietrabessa, M. Raimondi, E. Di Martino, Wear of polyethylenecups in total hip arthroplasty: a parametric mathematical model, *Medical Engineering & Physics* 20 (1998) 199-210

[7] T. Maxian, T. D. Brown, R. D. Pederson,J.J. Callaghan, A sliding distance coupled finite element formulation for polyethylene wear in total hip arthroplasty, *J. Biomechanics* 29 (1996) 687-692.

[8] J. Scholten, H. Haensel, N. Krekeler, H. Fuchs, R. Stenke, MH. Ejtehadi, Modellierung des Einflusses der Verschleissverteilung auf die Beanspruchung von Fachwerksgelenken,*Material Testing* 52 (2010) 463-469.

[9] P. Samyn, P. de Baets, Friction and Wear of acetal: a matter of scale, *Wear* 259 (2005) 697-702

[10] P. Samyn and P. de Baets, Friction and polyoxymethylene homopolymer in highly loaded applications extrapolated from small scaled, *Tribology letters* 19 (2005) 177-189

[11] H. Benabdallah, Friction and wear of blended polyoxymethylene sliding against coated steel plates, *Wear* 253 (2003) 1239-1246

[12] H. Endo, E. Marui, Effect of the specimen geometry on wear – combination of polyacetal (POM) and carbon steel for machine structures, *Wear* 258 (2005) 1525-1530